Region-specific wax tracers enable geographical origin tracing of Schisandra sphenanthera fruits via GC/MS chemotyping

Yiqing Luo, Lei Hu, Kai Chen, Junyu Xu, Mengting Xiao, Shimeng Li, Yiying Yang, Ying Wang, Zhaoqi Xie, Shaohua Zeng, Chunsong Cheng

PII: S2590-1575(25)01321-5

DOI: https://doi.org/10.1016/j.fochx.2025.103474

Reference: FOCHX 103474

To appear in: *Food Chemistry: X*

Received date: 11 October 2025

Revised date: 26 December 2025

Accepted date: 29 December 2025

Please cite this article as: Y. Luo, L. Hu, K. Chen, et al., Region-specific wax tracers enable geographical origin tracing of Schisandra sphenanthera fruits via GC/MS chemotyping, *Food Chemistry: X* (2024), https://doi.org/10.1016/j.fochx.2025.103474

Region-Specific Wax Tracers Enable Geographical Origin Tracing of *Schisandra sphenanthera* Fruits via GC/MS Chemotyping

Yiqing Luo[a b c ǂ], Lei Hu[a b ǂ], Kai Chen[a b], Junyu Xu[a b], Mengting Xiao[a b], Shimeng Li[a b], Yiying Yang[a b], Ying Wang[c], Zhaoqi Xie[a b], Shaohua Zeng[c *], Chunsong Cheng[a b *]

[a] *Jiangxi Key Laboratory for Sustainable Utilization of Chinese Materia Medica Resources, Lushan Botanical Garden, Chinese Academy of Science, Jiujiang City, Jiangxi Province, 332900, PR China*

[b] *Lushan Xinglin Institute for Medicinal Plants & Jiujiang Xinglin Key Laboratory for Traditional Chinese Medicines, Lushan, Jiujiang City, Jiangxi Province, 332900, PR China*

[c] *Guangdong Provincial Key Laboratory of Applied Botany, South China Botanical Garden, Chinese Academy of Sciences (Joint post-doctoral plan with Jiangxi Key Laboratory for Sustainable Utilization of Chinese Materia Medica Resources), Guangzhou City, Guangdong Province, 510650, PR China*

ǂThese authors contributed equally to this work.

***Corresponding authors**

Chunsong CHENG (chengcs@lsbg.cn) and Shaohua ZENG (shhzeng@scbg.ac.cn)

Abstract

Schisandra sphenanthera fruit, a popular wild berry widely used for beverages industrial material in northeast Asian regions, urgently requires origin tracing technologies for adapting to the market rule of 'better quality, better price'. This study first employed gas chromatography-mass spectrometry to analyze the cuticular wax of *S. sphenanthera* fruits from three main ecologically distinct production areas in China. The results showed that high levels of fatty acids (FA) and long-chain primary alcohols (LPA, C⩾26) were detected in the southwestern region (FA: 2.66 μg/cm² and LPA: 2.02 μg/cm²); The highest aldehyde (2.12 μg/cm²) and lowest sterol (0.50 μg/cm²) content were detected from the central region; The lowest total wax (14.52 μg/cm²) and higher sterol content (0.16 μg/cm²) were detected in the

eastern region. This study provided five indicative wax tracers firstly that serve as geographical indicators, enhancing knowledge of their ecological adaptability while establishing traceable chemical markers for geographical origin tracing.

Keywords: Schisandra sphenanthera fruit; Cuticular wax; Ecological adaptation; Chemical biomarkers; Geographical tracing

1. Introduction

Schisandra sphenanthera Rehd. et Wils (*S. sphenanthera*) fruit (*SF*) has emerged as a highly popular functional fruit in recent years, celebrated for its hepatoprotective, antioxidant, and anti-tumor activities [1-4]. The surface of *SF* is covered by a thick cuticular wax layer, serving as its hydrophobic barrier that plays a pivotal role in resisting environmental stresses such as drought, UV radiation, pathogen invasion, and regulating physiological processes. Previous studies have shown that cuticular waxes, primarily composed of long-chain fatty acids (LCFAs) and their derivatives (e.g., alkanes, alcohols, esters), exhibit remarkable plasticity in response to climatic variations [5-8]. However, the geographic variation in wax composition of *SF* across different ecological regions in China remains unexplored, hindering our understanding of their adaptive strategies and quality evaluation.

Cuticular wax biosynthesis is genetically and environmentally regulated [9,10]. In *Brassica napus*, drought and heat stresses alter wax composition, with C28 fatty acids, C29 primary alcohols, and C30 alkanes emerging as key stress-responsive components [11,12]. Similarly, in *Vicia faba*, organ-specific wax profiles (e.g., leaf, stem, petal) reflect functional adaptations, such as water retention in leaves and pollinator attraction in petals [13]. These findings imply that *SF* from distinct climatic zones may exhibit divergent wax profiles, potentially linked to local environmental pressures (e.g., temperature, precipitation, UV intensity) [7,14].

In economically significant species, geographic variation in cuticular waxes not only reflects ecological adaptation but also serves as a chemical "fingerprint" for quality control—a feature underexploited in wild berry plants despite its commercial and scientific potential. Geographic variation in plant cuticular waxes has been linked to ecological adaptation and

fruit quality [15]. For instance, in *SF*, lignans (major bioactive compounds) correlate with wax-associated stress tolerance [2,4]. Additionally, wax components like C29 alkane and secondary alcohols may influence the accumulation of bioactive metabolites[5,12,16]. Thus, characterizing wax profiles across *S. sphenanthera* habitats could reveal chemical markers for quality control and provide insights into the genetic basis of stress resistance.

In summary, while cuticular wax plasticity under environmental stress has been documented in model plant systems, the geographical variation of wax profiles in functional fruits plant like *S. sphenanthera* across China's diverse eco-climatic zones remains uncharted. Two critical gaps remain unresolved for economically important wild berry plant like *S. sphenanthera*: (1) the lack of systematic correlation between region-specific wax chemotypes and China's diverse eco-climatic gradients, and (2) the absence of verifiable wax biomarkers for geographical authentication. This study bridges this critical knowledge gap by conducting the first comprehensive GC-MS analysis of cuticular wax composition in *SF* from six major production provinces spanning subtropical to temperate monsoon climates. We find that distinct regional wax chemotypes emerge as adaptive responses to specific environmental pressures—particularly UV radiation, precipitation gradients, and diurnal temperature extremes—and that these chemical signatures can serve as robust biomarkers for geographical authentication and quality assessment. The integration of GC-MS based wax chemotyping with ecological factor analysis offers a novel framework for studying ecotype adaptation in wild berry plants. The identified wax chemotypes (e.g., aldehydes for drought tolerance, sterols for pathogen defense) can be directly implemented in supply chain traceability systems to authenticate geographical origins.

2. Materials and Methods

2.1. Reagents

Chloroform was purchased from General-Reagent (Shanghai, China). Pyridine, tetracosane, anhydrous sodium sulfate, N,O-Bis (trimethylsilyl) trifluoroacetamide (BSTFA), and 2-chloro-L-phenylalanine were obtained from Aladdin (Shanghai, China). Acetonitrile and methanol were sourced from Thermo (Loughborough, UK), while formic acid was supplied by TCL (Shanghai, China), and ammonium formate was supplied by Sigma

(Shanghai, China). Nitrogen gas was procured from Liufang Industrial Gas Co., Ltd (Suzhou, China).

2.2 Sample Collection

During autumn 2023, *SF* was harvested from six major production areas in China: Dali City (Yunnan Province), Guang'an City (Sichuan Province), Guilin City (Guangxi Province), Shangluo City (Shaanxi Province), Nanyang City (Henan Province), and Hefei City (Anhui Province). The selected plants from these production areas had been growing in consistent site conditions over several years, yielding medium-sized *SF*. Samples from these areas were labeled as YN, GX, SC, SX, HN, and AH, respectively.

After harvesting, the *SF* were dried at 45 ± 2.0 °C and stored in a cool environment. Each batch was divided into three subgroups, with six undamaged fruits selected from each subgroup for cuticular wax extraction. The diameter of each *SF* was measured using a caliper (both transverse and longitudinal diameters were recorded three times each) to calculate the cuticular area based on a spherical model.

For wax extraction, each subgroup was immersed in 6 mL of chloroform for 2 min. Anhydrous sodium sulfate (1 g) was added to the extract, and impurities were removed using neutral filter paper. The extract was then dried with nitrogen gas to obtain the wax-dried extract. The dried extract was dissolved and derivatized in pyridine and N,O-Bis (trimethylsilyl) trifluoroacetamide (BSTFA) at 70.0 ± 2.0 °C for 30 min. Finally, the sample was diluted with chloroform and analyzed using GC-MS.

2.3. GC-MS Detection of Wax Extracts

GC-MS analysis was performed using a gas chromatograph equipped with a mass spectrometric detector (m/z 50–750, MSD 5975; Agilent Technologies, Colorado Springs, U.S.A) and a capillary column (30 m × 0.32 mm, DB-1 ms, 0.1 μm film; J&W Scientific, Agilent Technologies, Colorado Springs, U.S.A). A 1 μL aliquot of each sample was injected into the system. The chromatographic temperature program was set as follows: an initial temperature of 50 ± 1.0 °C, held for 2 min, followed by a ramp of 40 ± 0.5 °C/min to 200 ± 1.0 °C, held for 2 min, increased at 3 ± 0.5 °C/min to 320 ± 1.0 °C, and maintained at 320 ± 1.0 °C for 30 min [17,18].

Retention times were compared and evaluated using the Wiley 10th/National Institute of Standards and Technology (NIST) 2017 Mass Spectral Library (W10N14; John Wiley & Sons) and LipidWeb data (https://www.lipidhome.co.uk/). Peak intensity signals were segmented and normalized based on internal standards, with an RSD > 0.3. After normalization, redundant signals were removed, and peak merging was performed to generate a refined data matrix. The obtained GC-MS data were then used to determine the wax content. This information, combined with the measured cuticular area, was utilized to calculate the wax content per unit cuticular area for wax scales from different production areas. The formula is as follows:

$$s = 4\Pi r^2 \quad (1)$$

$$c = m/(s_1 + s_2 + s_3 + s_4 + s_5 + s_6) \quad (2)$$

where r represents the average value of the transverse and longitudinal diameter of the *SF* (cm), s represents the cuticular area of the *SF* (cm^2), $s_{1\text{-}6}$ represent the cuticular areas of six *SF* in each group (cm^2), m represents the mass of wax components in different groups (μg), and c represents the wax concentration per unit cuticular area of the *SF*—that is, the wax content on the cuticular of the *SF* ($\mu g/cm^2$).

2.4 Acquisition of Climate and Environmental Factors

The map was acquired from National Geographic Information Public Service Platform (https://cloudcenter.tianditu.gov.cn/administrativeDivision), sunshine duration (SDU) and annual temperature range (ATR) data were sourced from China Meteorological Data Network (https://data.cma.cn/), annual precipitation (PRCP) date was obtained from National Earth System Science Data Center (http://www.geodata.cn).

2.5 Statistical Analysis

Each group conducted three biological replicates, and the results were expressed as the mean ± standard error. Inter-group difference was performed using one-way analysis of variance (ANOVA) with IBM SPSS Statistics (Version: 27, IBM company, Armonk, U.S.A), followed by Tukey' s HSD post hoc test for comparisons ($p < 0.05$).

3. Results and Discussion

3.1 Chemical Composition and Content Analysis of *SF* Cuticular Wax

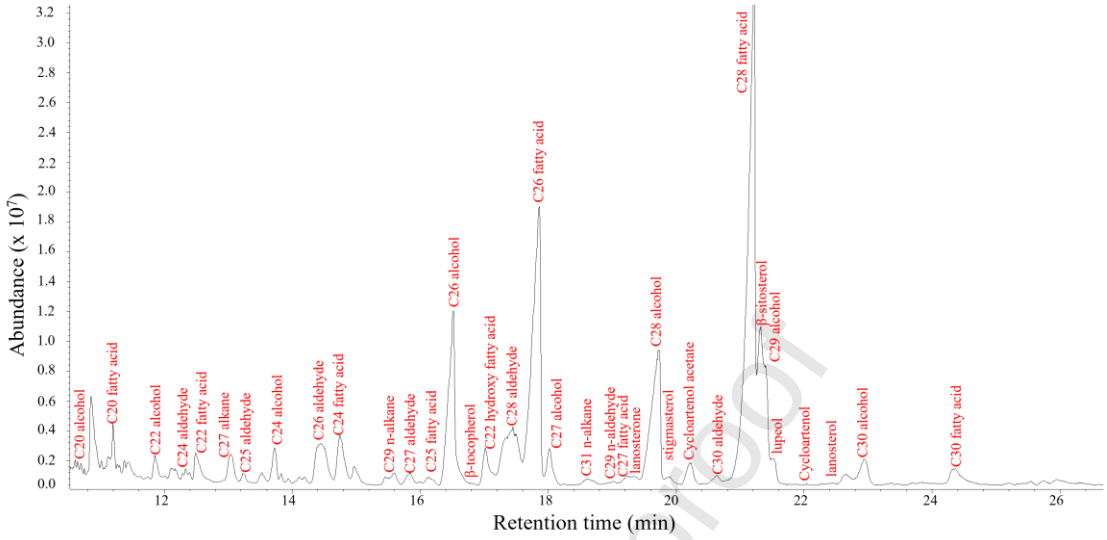

Fig. 1. GC-MS chromatogram of *SF* wax.

Cuticular wax was extracted from *SF* samples collected from various production areas and analyzed using GC-MS. The wax components were identified by comparing the obtained spectra with the NIST database (Fig. 1 and Table. 1). The wax components content of *SF* was calculated by combining the date of GC-MS with the cuticular area of *SF*.

Table. 1. The kinds of cuticular wax components on the *SF* surface and the retention time.

No.	Compound Abbreviation	Name	Retention Time (min)	Abundance (×10^7)
1	C20 alcohol	Eicosanol	10.45	0.23
2	C20 fatty acid	Eicosanoic acid (Arachidic acid)	11.18	0.42
3	C22 alcohol	Docosanol (Behenyl alcohol)	11.92	0.24
4	C24 aldehyde	Tetracosanal (Lignoceric aldehyde)	12.35	0.15
5	C22 fatty acid	Docosanoic acid (Behenic acid)	12.46	0.26
6	C27 n-alkane	Heptacosane	13.14	0.24
7	C25 aldehyde	Pentacosanal	13.13	0.12

8	C24 alcohol	Tetracosanol (Lignoceryl alcohol)	13.71	0.29
9	C26 aldehyde	Hexacosanal (Cerotic aldehyde)	14.44	0.32
10	C24 fatty acid	Tetracosanoic acid (Lignoceric acid)	14.67	0.37
11	C29 n-alkane	Nonacosane	15.58	0.11
12	C27 aldehyde	Heptacosanal	15.63	0.12
13	C25 fatty acid	Pentacosanoic acid	16.15	0.09
14	C26 alcohol	Hexacosanol (Ceryl alcohol)	16.5	1.21
15	β-tocopherol	β-tocopherol	16.78	0.05
16	C22 hydroxy fatty acid	22-Hydroxy docosanoic acid	17.03	0.28
17	C28 aldehyde	Octacosanal (Montanic aldehyde)	17.42	0.44
18	C26 fatty acid	Hexacosanoic acid (Cerotic acid)	17.83	1.91
19	C27 alcohol	Heptacosanol	18.22	0.28
20	C31 n-alkane	Heneicosane	18.63	0.08
21	C29 aldehyde	Nonacosanal	19.13	0.05
22	C27 fatty acid	Heptacosanoic acid	19.25	0.09
23	lanosterone	Lanosterone	19.42	0.08
24	C28 alcohol	Octacosanol (Montanyl alcohol)	19.73	0.93
25	stigmasterol	Stigmasterol	19.91	0.08
26	cycloartenol acetate	Cycloartenol acetate	20.31	0.18
27	C30 aldehyde	Triacontanal (Melissic aldehyde)	20.62	0.09
28	C28 fatty acid	Octacosanoic acid (Montanic acid)	21.13	3.24
29	β-sitosterol	β-sitosterol	21.34	1.09
30	C29 alcohol	Nonacosanol	21.42	0.84
31	lupeol	Lupeol	21.73	0.21
32	cycloartenol	Cycloartenol	22.05	0.04
33	lanosterol	Lanosterol	22.26	0.04
34	C30 alcohol	Triacontanol (Melissyl alcohol)	22.92	0.21
35	C30 fatty acid	Triacontanoic acid (Melissic acid)	24.37	0.14

3.2 Regional Differences Analysis of Cuticular Wax Components in *SF*

Screen out wax components showing significant differences ($p < 0.05$) among various *SF* origins and show in columnar diagrams with error bars indicating standard deviation (Fig.2).

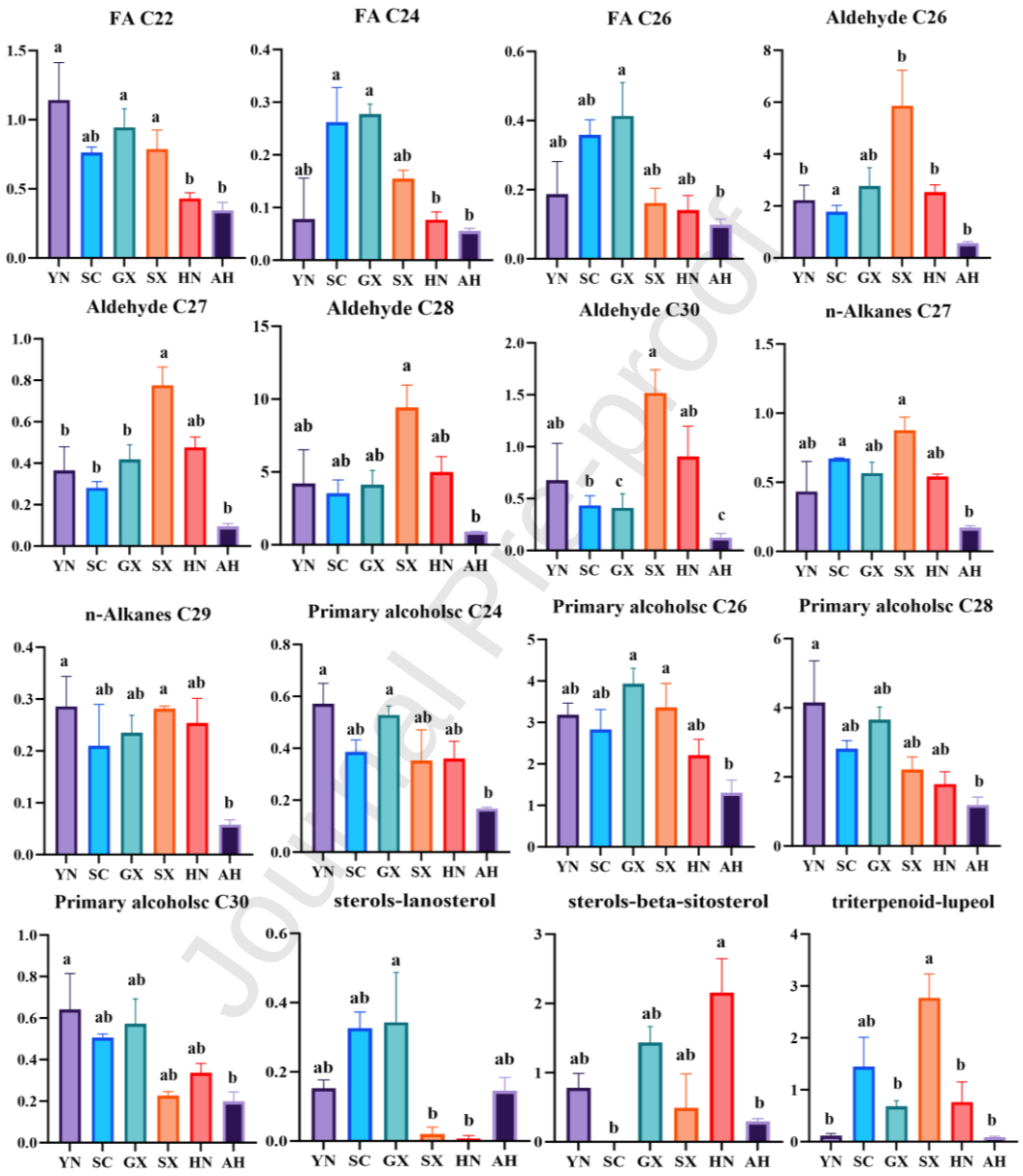

Fig. 2. Comparison of (a) hentriacontane, (b) n-tritriacontane, (c) n-pentatriacontane, (d) dotriacontane, and (e) n-tetratriacontane wax contents of *SF* from six production areas (YN, GX, SC, SX, HN, and AH). Different lowercase letters indicate significant differences, $p< 0.05$, Tukey' s HSD).

The Yunnan production area of *SF* is located at approximately 103°E longitude and falls

under a subtropical monsoon climate. The wax of *SF* here exhibits rich overall content, with the highest levels of fatty acid C22, primary alcohols C24, C28, and C30 (1.14, 0.57, 4.15, and 4.15 μg/cm², respectively). Conversely, the contents of fatty acids C24, C26, alkane C27, sterols-lanosterol, sterols-beta-sitosterol, and triterpenoid-lupeol are relatively low (0.08, 0.19, 0.43, 0.15, 0.78, and 0.08 μg/cm², respectively).

The Sichuan production area (longitude 104°E, subtropical monsoon climate) *SF* shows higher levels of fatty acids C24, C26, primary alcohol C30, and sterols-lanosterol (0.26, 0.36, 0.21, and 0.33 μg/cm², respectively). However, aldehydes (C26, C27, C28, C30) are present at lower levels (1.78, 0.28, 3.54, and 0.28 μg/cm², respectively), and sterols-beta-sitosterol is below detectable limits.

The Guangxi production area (longitude 108°E, also a subtropical monsoon climate) *SF* demonstrates higher contents of all fatty acids and primary alcohols compared to other regions, while aldehydes remain at lower levels.

The *SF* production area in Shaanxi is located at approximately 109°E longitude and falls under a temperate monsoon climate. Among the six major producing regions of *SF*, this area has the highest levels of aldehydes and triterpenes in its fruit wax (specifically, aldehyde C26, C27, C28, C30, and triterpene contents at 5.86, 0.78, 9.44, 1.52, and 2.77 μg/cm², respectively). The overall primary alcohol content is also relatively high, while sterols are comparatively low.

The Henan production area, situated at around 112°E longitude, also experiences a temperate monsoon climate. The composition of *SF* wax in Henan closely resembles that of Shaanxi, with similarly high aldehyde content and low fatty acid and sterols-lanosterol levels. Henan ranks second among the six regions in aldehyde content, just below Shaanxi. Notably, Henan has the highest sterols-beta-sitosterol content (measured at 2.16 μg/cm²) across all production regions.

Anhui, situated at approximately 117°E longitude, represents the easternmost production area among the six studied areas. Climatically, Anhui shares the subtropical monsoon climate characteristic with Yunnan, Sichuan, and Guangxi. However, cuticular wax accumulation in *SF* from Anhui was markedly lower compared to other regions. Quantitative analysis revealed that multiple wax components — including fatty acids, primary alcohols, and sterols —

consistently exhibited the lowest concentrations among all production areas examined in this study.

3.3 Regional Grouping of Cuticular Wax Chemotypes

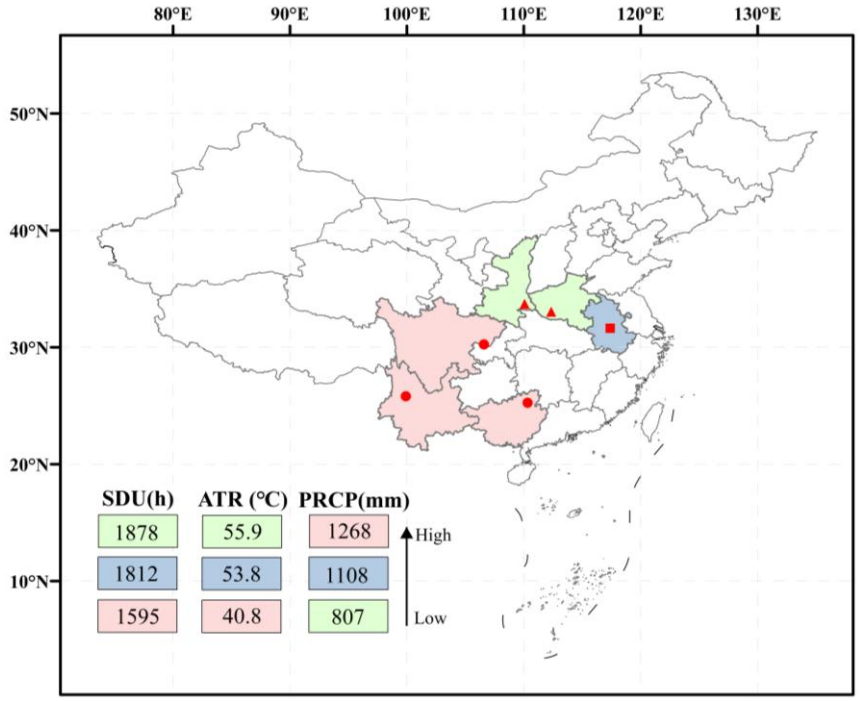

Fig. 3. The geographical locations of the six production areas of *SF*, as well as the sunshine duration (SDU), annual temperature range (ATR), and annual precipitation (PRCP) dates (the red background represents the southwest region, the green background represents the central region, and the blue background represents the eastern region).

Based on comprehensive analysis of climatic characteristics and cuticular wax composition patterns across different production regions, the six study locations were classified into three major groups to facilitate subsequent research and analysis14. The regional groupings were as follows: (1) southwestern group comprising Yunnan, Sichuan and Guangxi; (2) central group including Shaanxi and Henan; (3) eastern group represented by Anhui.

3.3.1 Southwestern Monsoon Adaptation: Fatty Acid and Primary Alcohol Dominance

The southwestern group, located in Southwest China's subtropical monsoon climate zone, exhibits strong similarities in *SF* cuticular wax composition patterns. Compared to other regions, this group demonstrates significantly higher contents of fatty acids and long-chain primary alcohols (carbon length > C26), with lower aldehyde concentrations. This primarily results from the group's climatic conditions - ample precipitation and moderate temperatures that promote plant growth and metabolism [15] (Fig. 3). These conditions facilitate the biosynthesis of more fatty acids (providing better fluidity and protective properties) and long-chain primary alcohols (carbon length > 26, which readily form dense "rod-like crystals" with superior stability and hydrophobicity compared to short-chain variants) rather than less stable aldehydes [19-21]. The "rod-like crystals" wax layer forms a protective membrane on fruit surfaces, preventing excessive water absorption and pathogen proliferation, and enhancing hydrophobicity against rain washout [15,19,22-24].

The humid, densely vegetated southwestern environment presents higher risks of pest/pathogen infestation and fruit infection compared to other regions [25-27]. Studies indicate that sterols-lanosterol could enhance fruit anti-inflammatory properties, effectively defending against pests/pathogens - explaining why the southwestern *SF* shows significantly higher sterols-lanosterol content [15,24,28,29].

Within the southwestern group, Yunnan *SF* shows slight differences in wax composition compared to Sichuan and Guangxi. Sichuan and Guangxi exhibit higher levels of fatty acids C24, C26, and sterols-lanosterol, while their C22 content is lower than Yunnan's. This divergence stems from Yunnan's high-altitude growing conditions, where intense UV exposure forces *S. sphenanthera* to adjust its wax synthesis pathway to counteract UV stress (Fig. 3). Under strong UV exposure, *S. sphenanthera* reduces hydrophobic long-chain fatty acids (LCFAs) (e.g., alkanes and primary alcohols) to lower wax crystallinity, forming more flexible short-chain structures that mitigate oxidative stress [5,9,30,31]. This is the reason that *S. sphenanthera* preferentially synthesizes short-chain fatty acids over long-chain ones to resist solar radiation. Regarding the content of sterols-lanosterol, Sichuan and Guangxi have very low levels, while Yunnan has significantly higher levels. These characteristics are also attributed to Yunnan high-altitude environment, where the climate is drier than that of Sichuan

and Guangxi. Consequently, due to lower humidity, *SF* in Yunnan faces a reduced risk of diseases and pests [15,25,32-34].

3.3.2 Central Aridity Response: Aldehyde and Triterpenoid Accumulation

SF from Shaanxi and Henan provinces in the central region exhibited remarkably similar wax compositions, with consistently lower fatty acid content and higher aldehyde levels. These provinces, located at relatively higher longitudes, experience a temperate monsoon climate characterized by cold, dry winters and hot summers (Fig. 3). *S. sphenanthera* in these regions appear to modify their wax biosynthesis strategies to adapt to large temperature variations and relatively arid conditions. Drought stress moderately suppressed fatty acid synthesis pathways, leading to increased aldehyde accumulation that enhances cuticular transpiration resistance [11]. The production of fatty acids, serving as wax precursors, is constrained by metabolic resource allocation under water stress conditions [9,11,33]. Additionally, high summer temperatures in the central region inhibit fatty acid elongase activity, significantly reducing long-chain fatty acid (LCFA) synthesis [5,9,11,16,33-36]. This was clearly demonstrated by the progressive decrease in relative fatty acid content with increasing carbon chain length in Shaanxi and Henan *SF* waxes. Furthermore, elevated temperatures promote aldehyde synthesis and accumulation, which contributes to cellular membrane stabilization [22,31]. Intense ultraviolet radiation accelerates LCFA oxidation, converting them into more chemically stable aldehydes. This explains the characteristically high aldehyde content in the surface waxes of Shaanxi and Henan *SF*, a phenomenon similarly observed in Yunnan province of the southwestern region [5,16]. Specifically, Yunnan's high-UV environment exhibited lower LCFA levels compared to Sichuan and Guangxi within the same regional group, while demonstrating slightly higher aldehyde content.

Moreover, the arid growing conditions of the central group's *S. sphenanthera* result in lower risks of pests, diseases, and inflammatory stress, reducing the need for plants to synthesize highly anti-inflammatory wax components [37,38]. As previously noted, the content of sterols-lanosterol correlates with the fruit's anti-inflammatory and pest-resistant properties. This is the primary reason for the low sterols-lanosterol levels observed in the

central group's *SF*. Within the central group, subtle differences in wax composition were observed between *SF* from Shaanxi and Henan. *SF* wax from Shaanxi exhibits significantly higher triterpenoid-lupeol content compared to that from Henan, and Henan *SF* wax show markedly elevated sterols-beta-sitosterol levels compared to Shaanxi. This divergence is closely linked to the ecological adaptation of *S. sphenanthera* across different production regions, where environmental factors such as soil composition differentially influence the biosynthetic pathways of these metabolites. In Shaanxi's Loess Plateau, characterized by nutrient-poor soil and poor water retention, plants reduce degradable fatty acids and increase antioxidant triterpenoid-lupeol to cope with environmental stress [34]. Conversely, Henan's transitional climate likely drives *S. sphenanthera* to enhance sterols-beta-sitosterol as a substitute for fatty acids in membrane stabilization. This adaptation reduces fatty acid demand in waxes, enabling the plant to maintain cellular membrane functionality under large diurnal temperature fluctuations, ensuring normal growth and metabolism [39].

3.3.3 Eastern Pathogen Defense Strategy: Sterol-Mediated Protection

In the Anhui producing area of eastern China, the overall *SF* wax component content is relatively low. *SF* from Anhui occupies a unique geographical location characterized by minimal diurnal and seasonal temperature variations, suitable sunlight exposure, and fertile soil (Fig. 3). These factors result in reduced environmental stress during plant growth, prompting *S. sphenanthera* to adopt more efficient adaptation strategies (e.g., resource allocation to growth/reproduction) rather than synthesizing abundant wax compounds. This aligns with the metabolic cost hypothesis under low environmental stress [10-12]. Notably, the eastern group exhibits higher sterols-lanosterol content, indicating that Anhui *S. sphenanthera* faces significant pest/pathogen and inflammatory stress, similar to the southwestern group.

3.4 Wax Carbon Chain Length: *S. sphenanthera* Growth Environmental Indicator

To elucidate functional differences in the cuticular wax of *SF* across three regions, this study analyzed the average carbon chain lengths (ACL) of various wax components (Fig. 4). The southwestern and eastern groups exhibited longer fatty acid ACLs (12.961 and 12.912,

respectively) compared to the central group (12.685), suggesting that the southwestern and eastern groups require enhanced synthesis of long-chain fatty acids to mitigate rain erosion damage (Fig. 4a). In contrast, the central group showed longer aldehyde ACLs (14.511) than the southwestern (14.455) and eastern groups (14.404), indicating greater need for UV resistance (Fig. 4b). For n-alkanes, the southwestern and central groups displayed significantly longer ACLs than the eastern group, demonstrating their adaptation to colder climates through increased long-chain alkane production to prevent frost damage (Fig. 4c). The southwestern group had the highest primary alcohol ACL in Fig. 4d (13.048), while the central group had the lowest (12.974). Since primary alcohol carbon length > C24 are known to reduce pathogen attachment and enhance defense, this implies higher pathogen pressure in the southwestern region and minimal risk in the central area.

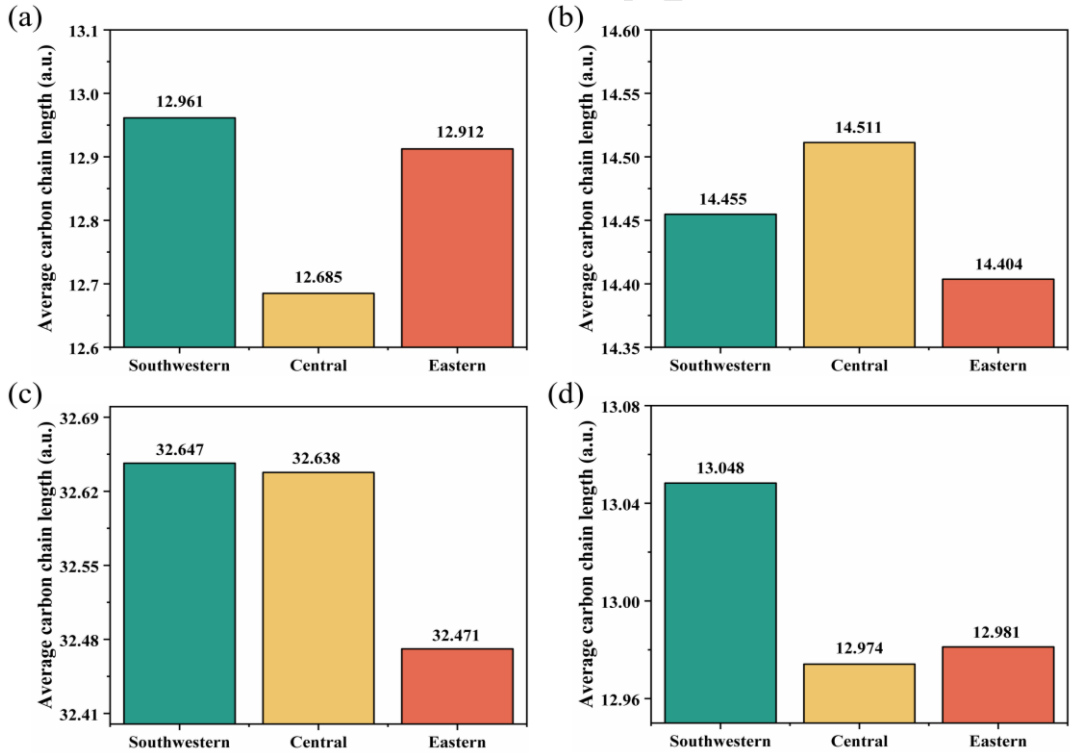

Fig. 4. Average carbon chain length of (a) total fatty acid, (b) total aldehyde, (c) total n-alkane, and (d) total primary alcohol in southwestern (green bar), central (yellow bar), and eastern (red bar) regions.

3.5 Correlation Heatmap Analysis of Cuticular Wax Components

The correlation heatmap of wax components from six major production regions was shown in Fig.5. Firstly, the results revealed strong positive correlations within each wax

category (e.g., primary alcohols with primary alcohols and fatty acids with fatty acids). Fatty acids and primary alcohols (the blue-highlighted waxes) showed a distinct regional specificity in southwest group, where their concentrations presented a significantly higher than other regions, and the strong mutual correlation in fatty acids and primary alcohols indicated a synergistic roles in biological defense and structure formation. Aldehydes (orange-highlighted) demonstrated specificity in central origin for chemical defense against extreme harsh weather conditions, correlating with the region's unique climatic conditions (large annual temperature variation, low precipitation, and intense sunlight). In contrast, aldehydes wax exhibit strong negative correlations with fatty acids and primary alcohols (southwest-specific wax), reflecting significant chemical feedback differences in *S. sphenanthera* surface chemistry across climatic zones. Eastern group show lower total wax content without region-specific components, though lanosterol (green-highlighted) concentrations are relatively higher. The *S. sphenanthera* from the eastern group experiences relatively mild environmental stresses and grows under favorable conditions. However, such an environment also facilitates insect reproduction and increases the incidence of fruit infections. Consequently, the eastern group *SF* relies more on lanosterol to mitigate these risks. Interestingly, lanosterol shows a weak negative correlation with aldehydes but slight positive correlations with selected fatty acids, n-alkanes, and primary alcohols. This suggests that in arid/high-UV regions, *S. sphenanthera* prioritizes aldehyde-rich waxes for water retention and UV protection, reducing reliance on lanosterol due to minimal pest/disease pressure in dry climates. By contrast, in humid environments, *S. sphenanthera* synthesizes hydrophobic waxes (fatty acids, n-alkanes, primary alcohols) to repel moisture, while simultaneously upregulating lanosterol synthesis to combat pathogen stresses driven by high humidity. This divergence reflects climate-driven metabolic trade-offs: aldehydes dominate under drought, whereas lanosterol synergizes with hydrophobic waxes in wet regions to address biotic threats. This results further demonstrates that *S. sphenanthera* exhibits diverse feedback mechanisms in response to varying climatic conditions.

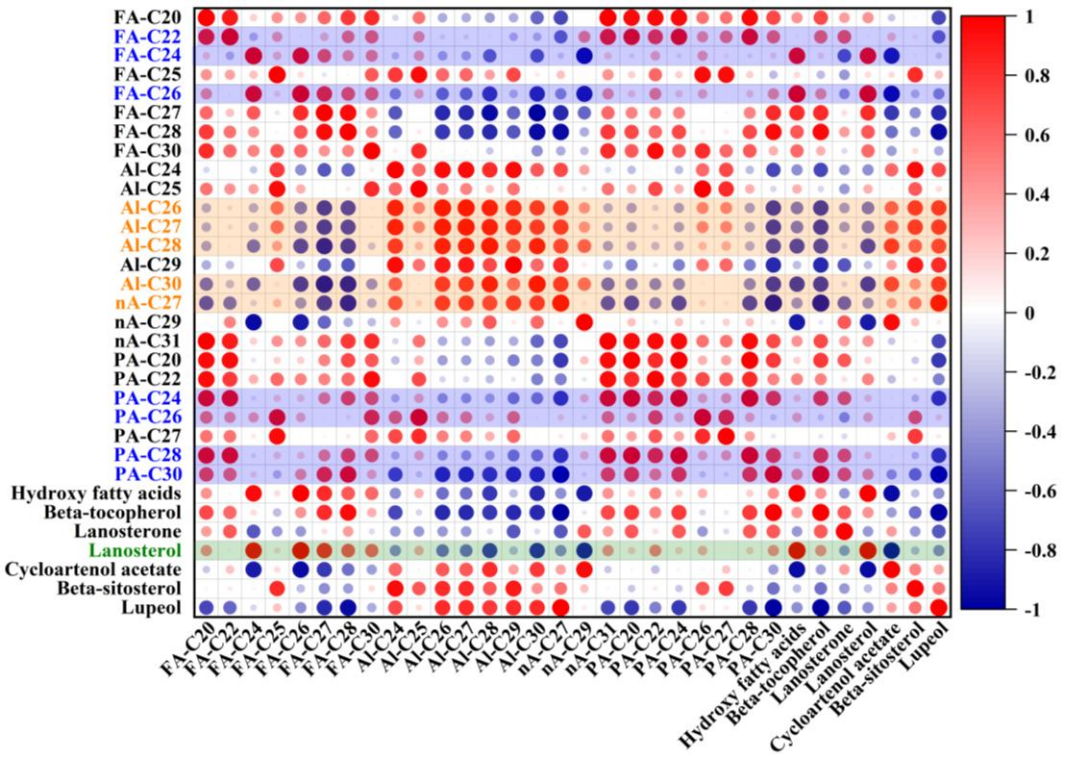

Fig. 5. Correlation heatmap of *SF* wax components across six *S. sphenanthera* production regions (the heatmap highlights region-specific wax profiles: blue for southwestern group, orange for central group, and green for eastern group. FA: fatty acid, Al: aldehyde, nA: n-alkane, PA: primary acohol).

4. Conclusion

This study provides the first chemical evidence for geographical divergence in the cuticular wax composition of *SF* across six Chinese provinces. Analysis via GC-MS revealed distinct regional patterns: the southwestern group (Yunnan, Sichuan, Guangxi) displayed dominance of long-chain fatty acids (e.g., C22) and primary alcohols (carbon length > 26), adaptations to high humidity and UV radiation ; the central group (Shaanxi, Henan) accumulated aldehydes (e.g., C28 aldehyde at 0.977 μg/cm²) and triterpenoids like lupeol, responses to arid conditions and temperature fluctuations; while the eastern group (Anhui) exhibited minimal total wax but elevated sterols (e.g., β-sitosterol), suggesting reduced abiotic stress but enhanced pest/pathogen and fruit ogenanti-inflammatory defense. This study advance understanding of ecological adaptability and establish reliable biomarkers for origin tracing and quality assessment of *SF*.

5. Research Outlook

5.1 Marker Validation & Expansion

While this study identified five candidate wax tracers, their robustness needs verification across: (i) more production regions (e.g., northeastern China), (ii) inter-annual climatic variations, and (iii) different cultivation practices. A longitudinal study spanning 3–5 years would clarify the temporal stability of these biomarkers.

5.2 Mechanism Exploration

The regulatory networks linking climatic factors to wax biosynthesis remain unresolved. Targeted transcriptomics and mutant analyses could decipher how environmental signals trigger region-specific wax patterning in *S. sphenanthera*.

5.3 Technology Translation

To bridge laboratory findings with industry needs, developing rapid detection methods is critical. Portable Reverse Transcription Polymerase Chain Reaction kits for wax-related gene expression or hyperspectral imaging paired with AI could enable real-time origin authentication at supply chain nodes.

CRediT authorship contribution statement

Yiqing Luo: Conceptualization, Investigation, Writing—original draft. **Lei Hu**: Conceptualization, Formal analysis. **Kai Chen**: Investigation, Data curation. **Junyu Xu**: Software, Writing – original draft. **Mengting Xiao**: Formal analysis, Data curation. **Shimeng Li**: Formal analysis. **Yiying Yang**: Formal analysis. **Ying Wang**: Conceptualization, Investigation, Project administration. **Zhaoqi Xie**: Conceptualization, Data curation. **Chunsong Cheng**: Formal analysis, Writing—original draft, Writing—review & editing, Conceptualization, Supervision, and Funding acquisition. **Shaohua Zeng**: Writing—review & editing, Supervision.

Acknowledgment

The study was supported by Jiangxi Province Double Thousand Talent-Leader of Natural Science Project (jxsq2023101038), Jiangxi Province Urgently Overseas Talent Project

(2022BCJ25027), The Key Research Projects in Jiangxi Province (20223BBH8007 & 20232BBG70014), Jiujiang Xinglin Key Laboratory for Traditional Chinese Medicines (S2024ZDSYS037), and Youth Innovation Promotion Association CAS (2015286).

References:

[1] Yang, K., Qiu, J., Huang, Z., Yu, Z., Wang, W., Hu, H., & You, Y. (2022). A comprehensive review of ethnopharmacology, phytochemistry, pharmacology, and pharmacokinetics of *Schisandra chinensis* (Turcz.) Baill. and *Schisandra sphenanthera* Rehd. et Wils. *Journal of Ethnopharmacology*, 284, 114759. https://doi.org/10.1016/j.jep.2021.114759

[2] Mou, Q., He, J., Li, X., Yang, B., Yang, L., & Li, H. (2018). Rapid discrimination of *Schisandra sphenanthera* and *Schisandra chinensis* using electronic tongue and ultra-performance liquid chromatography coupled with chemometrics. *Acta Ecologica Sinica*, 38(3), 193-199. https://doi.org/10.1016/j.chnaes.2017.11.004

[3] Liu, D., Yang, K., Li, T., Tang, T., Wang, Y., Wang, W., Li, J., Zhou, P., Wang, X., Zhao, C., Guo, D., Xie, Y., Cheng, J., Wang, M., Sun, J., & Zhang, X. (2024). The protective effects of aqueous extract of *Schisandra sphenanthera* against alcoholic liver disease partly through the PI3K-AKT-IKK signaling pathway. *Heliyon*, 10(13), e34214. https://doi.org/10.1016/j.heliyon.2024.e34214

[4] Bansal, S., Pratiksha, K., Gaur, R., Gupta, S., Jadaun, V. P., & Kumari, V. (2024). Comprehensive review on *Schisandra chinesis*. *Pharmacological Research - Modern Chinese Medicine*, 10, 100406. https://doi.org/10.1016/j.prmcm.2024.100406

[5] Zhao, P., Li, Q., Lei, Y., Zou, J., & Li, Q. (2025). Adaptation of cuticle metabolism to abiotic stress in plants. *Crop and Environment*, 4(1), 38-44. https://doi.org/10.1016/j.crope.2025.01.001

[6] Xu, D., Qi, C., Yang, J., Ni, Y., & Guo, Y. (2024). The cuticular wax on sorghum straw influenced soil microbial diversity and straw degradation in soil. *Applied Soil Ecology*, 195, 105272. https://doi.org/10.1016/j.apsoil.2024.105272

[7] Cerón-Carpio, A. B., Pérez-García, B., Monribot Villanueva, J. L., Kiel-Martínez, A. L.,

Espinosa-Matias, S., Guerrero-Analco, J. A., & Mehltreter, K. (2019). Chemical composition and micromorphological structure of cuticular leaf waxes of eight tropical fern species of Mexico. *Biochemical Systematics and Ecology*, 85, 13-20. https://doi.org/10.1016/j.bse.2019.04.008

[8] Luo, Y., Guo, M., Hu, L., Yang, J., Xu, J., Rafiq, M., Wang, Y., Cheng, C., & Zeng, S. (2025). Preliminary Study on the Geochemical Characterization of Viticis Fructus Cuticular Waxes: From Latitudinal Variation to Origin Authentication. *International Journal of Molecular Sciences*, 26(15), 7293. https://doi.org/10.3390/ijms26157293

[9] Peng, A., Zhang, J., Zhu, Y., Ye, Z., Chen, Z., He, Y., Li, Q., & Chen, S. (2024). CsFAO3 enhances citrus canker severity by regulating leaf cuticular wax production in *Citrus sinensis*. *Scientia Horticulturae*, 338, 113806. https://doi.org/10.1016/j.scienta.2024.113806

[10] Zhao, X., Xie, J., Yang, L., Hu, W., Song, J., Kuang, L., Huang, Y., Liu, Y., & Liu, D. (2025). CsRAP2-7 negatively regulates cuticular wax biosynthesis and drought resistance in citrus by directly activating CsACO1. *Plant Physiology and Biochemistry*, 224, 109983. https://doi.org/10.1016/j.plaphy.2025.109983

[11] Tomasi, P., Luo, Z., & Abdel-Haleem, H. (2024). Drought and high heat stresses modify *Brassica napus* L. leaf cuticular wax. *Plant Stress*, 13, 100513. https://doi.org/10.1016/j.stress.2024.100513

[12] Tassone, E. E., Lipka, A. E., Tomasi, P., Lohrey, G. T., Qian, W., Dyer, J. M., Gore, M. A., & Jenks, M. A. (2016). Chemical variation for leaf cuticular waxes and their levels revealed in a diverse panel of *Brassica napus* L. *Industrial Crops and Products*, 79, 77-83. https://doi.org/10.1016/j.indcrop.2015.10.047

[13] Zhao, X., Huang, L., Kang, L., Jetter, R., Yao, L. H., Li, Y., Xiao, Y., Wang, D. K., Xiao, Q. L., Ni, Y., & Guo, Y. J. (2019). Comparative analyses of cuticular waxes on various organs of faba bean (*Vicia faba* L.). *Plant Physiology and Biochemistry*, 139, 102-112. https://doi.org/10.1016/j.plaphy.2019.03.015

[14] Carvalho, J. C. S., Frazão, A., Lohmann, L. G., & Ferreira, M. J. P. (2021). Leaf cuticular waxes of *Tanaecium* (Bignonieae, Bignoniaceae): Chemical composition and taxonomic implications. *Biochemical Systematics and Ecology*, 98, 104325. https://doi.org/10.1016/j.bse.2021.104325

[15] Wu, W., Jiang, B., Liu, R., Han, Y., Fang, X., Mu, H., Farag, M. A., Simal-Gandara, J., Prieto, M. A., Chen, H., Xiao, J., & Gao, H. (2023). Structures and functions of cuticular wax in postharvest fruit and its regulation: A comprehensive review with future perspectives. *Engineering*, 23, 118-129. https://doi.org/10.1016/j.eng.2022.12.006

[16] Kunst, L., & Samuels, A. L. (2003). Biosynthesis and secretion of plant cuticular wax. *Progress in Lipid Research*, 42(1), 51-80. https://doi.org/10.1016/S0163-7827(02)00045-0

[17] Çelik, H. T., Vural, N., & Kaymak, S. (2025). SPME-GC-MS profiling of volatile compounds in *Lucilia sericata* larva extract and in silico biotherapeutic analysis. International Journal of Tropical Insect Science, 45(4), 741 – 749. https://doi.org/10.1007/s42690-025-01472-0

[18] Çelik, H. T., Vural, N., & Kaymak, S. (2025). Green synthesis and larvicidal activity of ZnO nanoparticles against *Lucilia sericata* larvae using essential oil bio-reductants. Veterinary Parasitology, 340, 110633. https://doi.org/10.1016/j.vetpar.2025.110633

[19] Koch, K., & Ensikat, H.-J. (2008). The hydrophobic coatings of plant surfaces: Epicuticular wax crystals and their morphologies, crystallinity and molecular self-assembly. *Micron*, 39(7), 759-772. https://doi.org/10.1016/j.micron.2007.11.010

[20] Peng, Z., Chen, H., Niu, B., Wu, W., Chen, H., Farag, M. A., Ding, Y., Liu, R., & Gao, H. (2025). Composition and micromorphological determination of blue honeysuckle fruit (*Lonicera caerulea* L.) cuticular wax and its effects on fruit post-harvest quality. *Food Chemistry*, 463, 141330. https://doi.org/10.1016/j.foodchem.2024.141330

[21] Lemieux, B. (1996). Molecular genetics of epicuticular wax biosynthesis. *Trends in Plant Science*, 1(9), 312-318. https://doi.org/10.1016/S1360-1385(96)88178-0

[22] Zhang, W., Wang, Y., Guo, H., Yang, W., Guo, M., & Chen, G. (2022). Cuticular wax removal on reactive oxygen species-related mechanisms and on the quality of Hami melon cultivars. *Postharvest Biology and Technology*, 193, 112060. https://doi.org/10.1016/j.postharvbio.2022.112060

[23] Min, D., Li, F., Wang, J., Fu, X., Ali, M., Song, Y., Ding, J., Li, X., Li, M., Yang, K., & Zhang, X. (2024). Transcriptome reveals insights into the regulatory mechanism of cuticular wax synthesis in developing apple fruit. *Scientia Horticulturae*, 328, 112891. https://doi.org/10.1016/j.scienta.2024.112891

[24] Wu, X., Yin, H., Chen, Y., Li, L., Wang, Y., Hao, P., Cao, P., Qi, K., & Zhang, S. (2017).

Chemical composition, crystal morphology and key gene expression of cuticular waxes of Asian pears at harvest and after storage. *Postharvest Biology and Technology*, 132, 71-80. https://doi.org/10.1016/j.postharvbio.2017.05.007

[25] Wang, L., & Teplitski, M. (2023). Microbiological food safety considerations in shelf-life extension of fresh fruits and vegetables. *Current Opinion in Biotechnology*, 80, 102895. https://doi.org/10.1016/j.copbio.2023.102895

[26] Zhu, Y., Guan, M., Jia, Q., Wang, G., Pan, L., & Li, Y. (2024). Degradation mechanism of cuticular wax composition and surface properties of bamboo culm during storage. *Industrial Crops and Products*, 214, 118558. https://doi.org/10.1016/j.indcrop.2024.118558

[27] Tello, M. L., Tomalak, M., Siwecki, R., Gáper, J., Motta, E., & Mateo-Sagasta, E. (2005). Biotic urban growing conditions — Threats, pests and diseases. In C. Konijnendijk, K. Nilsson, T. Randrup, & J. Schipperijn (Eds.), *Urban forests and trees* (pp. 325–365). Springer. https://doi.org/10.1007/3-540-27684-X_13

[28] Mudalungu, C. M., Mokaya, H. O., & Tanga, C. M. (2023). Beneficial sterols in selected edible insects and their associated antibacterial activities. *Scientific Reports*, 13, 10786. https://doi.org/10.1038/s41598-023-37905-4

[29] Liu, R., Zhang, L., Xiao, S., Chen, H., Han, Y., Niu, B., Wu, W., & Gao, H. (2023). Ursolic acid, the main component of blueberry cuticular wax, inhibits *Botrytis cinerea* growth by damaging cell membrane integrity. *Food Chemistry*, 415, 135753. https://doi.org/10.1016/j.foodchem.2023.135753

[30] Chu, W., Gao, H., Chen, H., Fang, X., & Zheng, Y. (2018). Effects of cuticular wax on the postharvest quality of blueberry fruit. *Food Chemistry*, 239, 68-74. https://doi.org/10.1016/j.foodchem.2017.06.024

[31] Zhang, C., Li, L., Zhang, Y., Liang, Q., Luo, S., Huang, Z., Li, H., Escalona, V. H., Chen, Z., Zhang, F., Tang, Y., & Sun, B. (2024). *BoaCRTISO* regulates the color and glossiness of Chinese kale through its effects on pigment, abscisic acid, and cuticular wax biosynthesis. *Horticultural Plant Journal*, Volume 10. https://doi.org/10.1016/j.hpj.2024.06.008

[32] Couey, H. M. (1989). Heat treatment for control of postharvest diseases and insect pests of fruits. *HortScience*, 24(2), 198–202. https://doi.org/10.21273/HORTSCI.24.2.198

[33] Huang, H., Liu, H., Wang, L., & Xiang, X. (2023). Cuticular wax metabolism responses to

atmospheric water stress on the exocarp surface of litchi fruit after harvest. *Food Chemistry*, 414, 135704. https://doi.org/10.1016/j.foodchem.2023.135704

[34] Wan, X., Lin, X., Zhang, Y., Luo, D., Peng, J., Huang, H., Ding, X., & Dong, X. (2024). Revealing the crucial role of cuticular wax components in postharvest chilling injury of plums (*Prunus salicina Lindl.*). *Scientia Horticulturae*, 338, 113843. https://doi.org/10.1016/j.scienta.2024.113843

[35] Kong, Q., Liu, R., Wu, W., Chen, H., Han, Y., Fang, X., Zhang, Y., Chen, H., Mu, H., Gao, H., & Chen, J. (2024). *VcMYB30* enhances wax production and maintains fruit quality by regulating cuticular wax biosynthesis genes. *Postharvest Biology and Technology*, 212, 112856. https://doi.org/10.1016/j.postharvbio.2024.112856

[36] Kunst, L., & Samuels, L. (2009). Plant cuticles shine: advances in wax biosynthesis and export. *Current Opinion in Plant Biology*, 12(6), 721-727. https://doi.org/10.1016/j.pbi.2009.09.009

[37] Pant, P., Pandey, S., & Dall'Acqua, S. (2021). The influence of environmental conditions on secondary metabolites in medicinal plants: A literature review. *Chemistry & Biodiversity*, 18(11), e2100345. https://doi.org/10.1002/cbdv.202100345

[38] Yang, L., Wen, K. S., Ruan, X., Zhao, Y. X., Wei, F., & Wang, Q. (2018). Response of plant secondary metabolites to environmental factors. *Molecules*, 23(4), 762. https://doi.org/10.3390/molecules23040762

[39] Jia, E., Dong, J., & Ma, P. (2023). A new industrial model: The utilization of the traditional Chinese herb *Schisandra chinensis* (Turcz.) Baill. from soil to plate. *Industrial Crops and Products*, 191(Part A), 115900. https://doi.org/10.1016/j.indcrop.2022.115900

Declaration of interests

☒The authors declare that they have no known competing financial interests or personal relationships that could have appeared to influence the work reported in this paper.

☐The authors declare the following financial interests/personal relationships which may be considered as potential competing interests:

Highlights

1 Geographic-specific fruit cuticular waxes enable reliable origin traceability;

2 Hexacosanal is first reported as a geographical marker for Schisandra sphenanthera;

3 Long-chain fatty acids and primary alcohols mediate adaptation to summer rainfall areas;

4 Elevated aldehydes enhance the fruit resilience to wide temperature shifts.